

Applied Mathematics and Nonlinear Sciences

<https://www.sciendo.com>**On the Method of Inverse Mapping for Solutions of Coupled Systems of Nonlinear Differential Equations Arising in Nanofluid Flow, Heat and Mass Transfer**Mangalagama Dewasurendra, Kuppapalle Vajravelu [†]*Department of Mathematics, University of Central Florida, Orlando, FL 32816-1364, USA***Submission Info**

Communicated by Juan L.G. Guirao
Received 12th November 2017
Accepted 5th February 2018
Available online 5th February 2018

Abstract

Very recently, Liao has invented a Directly Defining Inverse Mapping Method (MDDiM) for nonlinear differential equations. Liao's method is novel and can be used for solving several problems arising in science and engineering, if we can extend it to nonlinear systems. Hence, in this paper, we extend Liao's method to nonlinear-coupled systems of three differential equations. Our extension is not limited to single, double or triple equations, but can be applied to systems of any number of equations.

Keywords: Method of directly defining the inverse mapping; Nonlinear systems; Nanofluid; Brownian motion; Stretching surface; analytical methods; Homotopy analysis method.

AMS 2010 codes: 34A25, 34A34, 34B15, 65L10, 76D10.

1 Introduction

Consider a steady, incompressible, laminar, two-dimensional boundary layer flow of a nanofluid at a vertical wall coincide with the plane $y = 0$, the flow being confined to $y > 0$ (see Figure 1). Two equal and opposite forces are introduced along the x -axis so that the wall is stretched while keeping the origin fixed. The sheet is then stretched with a velocity $u_w = ax^n$ where a is a constant, n is a nonlinear stretching parameter and x is the coordinate measured along the stretching surface. We make following assumptions:

- (i) the pressure gradient and external forces are neglected
- (ii) the stretching surface is maintained at a constant temperature and concentration, T_w and C_w , respectively,
- (iii) T_w and C_w values are greater than the ambient temperature and concentration, T_∞ and C_∞ respectively.

[†]Kuppapalle Vajravelu.

Email address: kuppapalle.vajravelu@ucf.edu

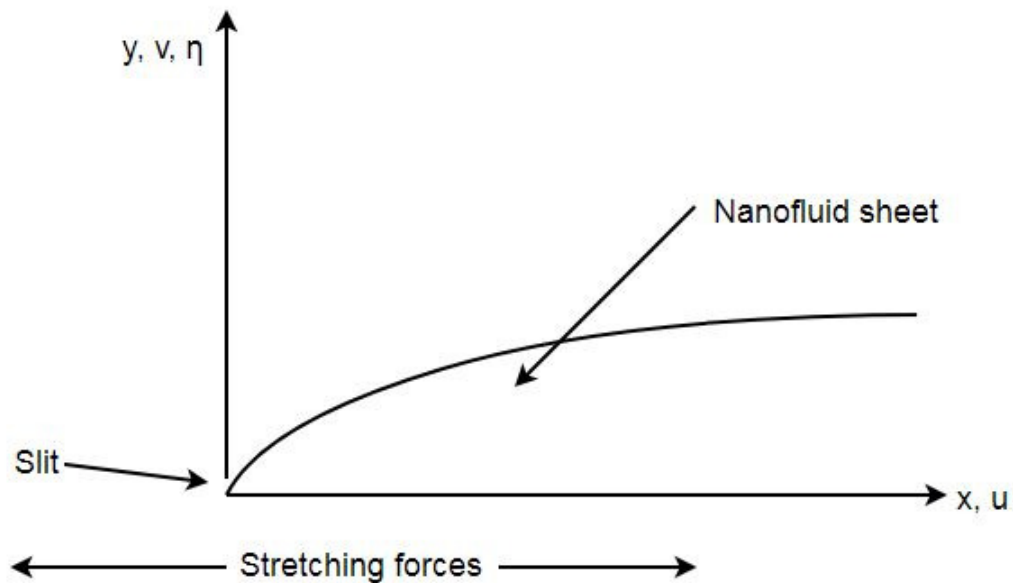


Fig. 1 Flow configuration.

Under these assumptions, the basic equations for the conservation of mass, momentum, thermal energy and nanoparticles of the nanofluid can be written in Cartesian coordinates x and y as (for details see Rana and Bhargava [1])

$$\frac{\partial u}{\partial x} + \frac{\partial v}{\partial y} = 0, \tag{1}$$

$$u \frac{\partial u}{\partial x} + v \frac{\partial u}{\partial y} = \nu \frac{\partial^2 u}{\partial y^2}, \tag{2}$$

$$u \frac{\partial T}{\partial x} + v \frac{\partial T}{\partial y} = \alpha_m \nabla^2 T + \tau \left[D_B \frac{\partial C}{\partial y} \frac{\partial T}{\partial y} + \frac{D_T}{T_\infty} \left(\frac{\partial T}{\partial y} \right)^2 \right], \tag{3}$$

$$u \frac{\partial C}{\partial x} + v \frac{\partial C}{\partial y} = D_B \frac{\partial^2 C}{\partial y^2} + \left(\frac{D_T}{T_\infty} \right) \frac{\partial^2 T}{\partial y^2}, \tag{4}$$

where

$$\alpha_m = \frac{k_m}{(\rho c)_f}, \quad \tau = \frac{(\rho c)_p}{(\rho c)_f}. \tag{5}$$

The boundary conditions for the problem are

$$v = 0, \quad u_w = ax^n, \quad T = T_w, \quad C = C_w \quad \text{at} \quad y = 0, \tag{6}$$

$$u = v = 0, \quad T = T_\infty, \quad C = C_\infty \quad \text{as} \quad y \rightarrow \infty. \tag{7}$$

Here u and v are the velocity in the x and y directions, ρ_f is the density of the base fluid, α_m is the thermal diffusivity, ν is the kinematic viscosity, a is a positive constant, D_B is the Brownian coefficient, D_T is the thermophoretic diffusion coefficient, τ is the ratio between the effective heat capacity of the nanoparticle material and heat capacity of the fluid, c is the volumetric volume expansion coefficient and ρ_p is the density of the nanoparticles.

Defining the new variables

$$\eta = y\sqrt{\frac{a(n+1)}{2v}}x^{\frac{n-1}{2}}, \quad u = ax^n f'(\eta), \quad v = -\sqrt{\frac{av(n+1)}{2}}x^{\frac{n-1}{2}}\left(f + \left(\frac{n-1}{n+1}\right)\eta f'\right), \quad (8)$$

$$\theta(\eta) = \frac{T - T_\infty}{T_w - T_\infty}, \quad \phi(\eta) = \frac{C - C_\infty}{C_w - C_\infty}, \quad (9)$$

and substituting in (1)-(4), we obtained

$$f''' + ff'' - \left(\frac{2n}{n+1}\right)f'^2 = 0, \quad (10)$$

$$\frac{1}{Pr}\theta'' + f\theta' + Nb\theta'\phi' + Nt(\theta')^2 = 0, \quad (11)$$

$$\phi'' + \frac{1}{2}Le f\phi' + \frac{Nt}{Nb}\theta'' = 0, \quad (12)$$

with boundary conditions,

$$\text{at } \eta = 0, \quad f = 0, \quad f' = 1, \quad \theta = 1, \quad \phi = 1, \quad (13)$$

$$\text{as } \eta \rightarrow \infty, \quad f' = 0, \quad \theta = 0, \quad \phi = 0. \quad (14)$$

The key thermophysical parameters are defined by:

$$Pr = \frac{v}{\alpha}, \quad Le = \frac{v}{D_B}, \quad Nb = \frac{(\rho c)_p D_B (C_w - C_\infty)}{(\rho c)_f v}, \quad Nt = \frac{(\rho c)_p D_T (T_w - T_\infty)}{(\rho c)_f v T_\infty}. \quad (15)$$

Here Pr, Le, Nb , and Nt denote the Prandtl number, the Lewis number, the Brownian motion parameter and the thermophoresis parameter respectively.

In the present paper, we study the nonlinear system analytically through the Optimam Homotopy Analysis Method by directly defining an inverse mapping \mathcal{J} , i.e. without calculating any inverse operator. This method was introduced by Liao [2] for a single differential equation. Vajravelu et al. [3] extended it to solve coupled systems. Here, we extend the method to a system of three nonlinear differential equations using a common inverse linear mapping and approximated $f(\eta)$, $\theta(\eta)$ and $\phi(\eta)$.

2 HAM and MDDiM

In this section, we discuss the set up of the problem using the details of OHAM (see [4]- [5] for more details) and MDDiM for the nonlinear system. First, we discuss the space that solution and base functions come from and then we derive deformation equations that we are trying to solve (nonlinear system). Finally, we use MDDiM to solve these deformation equations by introducing an appropriate inverse linear map \mathcal{J} .

Define three nonlinear operators

$$N_1[f(\eta), \theta(\eta), \phi(\eta)] = f''' + ff'' - \left(\frac{2n}{n+1}\right)f'^2, \quad (16)$$

$$N_2[f(\eta), \theta(\eta), \phi(\eta)] = \frac{1}{Pr}\theta'' + f\theta' + Nb\theta'\phi' + Nt(\theta')^2, \quad (17)$$

$$N_3[f(\eta), \theta(\eta), \phi(\eta)] = \phi'' + \frac{1}{2}Le f\phi' + \frac{Nt}{Nb}\theta'' = 0, \quad (18)$$

so that $N_1[f(\eta), \theta(\eta), \phi(\eta)] = 0$, $N_2[f(\eta), \theta(\eta), \phi(\eta)] = 0$ and $N_3[f(\eta), \theta(\eta), \phi(\eta)] = 0$ give the original system (10)-(12). Take complete set of an infinite number of base functions that are linearly independent

$$S_\infty = \{1, e^{-\delta\eta}, e^{-2\delta\eta}, \dots\}, \tag{19}$$

and define the space of functions that is their linear combinations to be

$$V = \left\{ \sum_{k=0}^{\infty} a_k e^{-k\delta\eta} \mid a_k \in \mathbb{R} \right\}. \tag{20}$$

That is, V is the solution and base space for $f(\eta)$, $\theta(\eta)$ and $\phi(\eta)$.

Let

$$S^* = \{1, e^{-\delta\eta}\}. \tag{21}$$

denote a set, consists of first 2 members of S_∞ . Next, form the space of functions taking their linear combinations

$$V^* = \{a_0 + a_1 e^{-\delta\eta} \mid a_0, a_1 \in \mathbb{R}\}. \tag{22}$$

Then the primary solutions, or our initial guesses, $\mu(\eta) \in V^*$ have the form

$$\mu(\eta) = \sum_{j=0}^1 a_j e^{-\delta\eta}. \tag{23}$$

Write

$$\widehat{S} = \{e^{-2\delta\eta}, e^{-3\delta\eta}, \dots\}, \tag{24}$$

and define

$$\widehat{V} = \left\{ \sum_{k=2}^{\infty} a_k e^{-k\delta\eta} \mid a_k \in \mathbb{R} \right\}. \tag{25}$$

Obviously, $V = \widehat{V} \cup V^*$.

Next, define

$$S_R = \{\psi_1(\eta), \psi_2(\eta), \dots\}, \tag{26}$$

which is an infinite set of base functions that are linearly independent, and set of linear combinations of functions from S_R

$$U = \left\{ \sum_{k=1}^{\infty} c_k \psi_k(\eta) \mid c_k \in \mathbb{R} \right\}. \tag{27}$$

Assuming that $N_1[f(\eta), \theta(\eta), \phi(\eta)], N_2[f(\eta), \theta(\eta), \phi(\eta)], N_3[f(\eta), \theta(\eta), \phi(\eta)] \in U$, then $N_1, N_2, N_3 : V \rightarrow U$.

Optimal Homotopy Analysis Method allows us to obtain approximate series solutions to wide variety of nonlinear systems. Define three homotopies of operators $\mathcal{H}_1, \mathcal{H}_2$ and \mathcal{H}_3

$$0 \equiv \mathcal{H}_1(f, \theta, \phi, q) = (1 - q)L_1[f] - c_0 q N_1[f, \theta, \phi], \tag{28}$$

$$0 \equiv \mathcal{H}_2(f, \theta, \phi, q) = (1 - q)L_2[\theta] - c_1 q N_2[f, \theta, \phi], \tag{29}$$

$$0 \equiv \mathcal{H}_3(f, \theta, \phi, q) = (1 - q)L_3[\phi] - c_2 q N_3[f, \theta, \phi], \tag{30}$$

through the homotopy embedding parameter $q \in [0, 1]$, between nonlinear operators N_1, N_2, N_3 and an auxiliary linear operators L_1, L_2, L_3 . Here, $c_0, c_1, c_2 \neq 0$ are the converge control parameters which will be used to optimize

the function approximations in the next section. In the frame of OHAM, the series solution of f, θ and ϕ is given by

$$f(\eta) = f_0(\eta) + \sum_{k=1}^{\infty} f_k(\eta)q^k, \tag{31}$$

$$\theta(\eta) = \theta_0(\eta) + \sum_{k=1}^{\infty} \theta_k(\eta)q^k, \tag{32}$$

$$\phi(\eta) = \phi_0(\eta) + \sum_{k=1}^{\infty} \phi_k(\eta)q^k, \tag{33}$$

where $f_0(\eta), \theta_0(\eta)$ and $\phi_0(\eta)$ are initial guesses that satisfy boundary conditions (13)-(14) and belong to the set V .

It is clear that when $q = 0$ in the homotopies (28)-(30), they become $L_1[f] = 0, L_2[\theta] = 0$ and $L_3[\phi] = 0$; but for $q = 1$, the original nonlinear differential equations $N_1[f, \theta, \phi] = 0, N_2[f, \theta, \phi] = 0$ and $N_3[f, \theta, \phi] = 0$ are recovered. In addition, when $q = 1$ in the expansions (31)-(33), the solutions f, θ and ϕ are a sum of the components $f_0, f_1, f_2, \dots, \theta_0, \theta_1, \theta_2, \dots$ and $\phi_0, \phi_1, \phi_2, \dots$. Substituting (31)-(33) in to the first homotopy (28), we get the deformation equations

$$L_1[f_0(\eta)] = 0, \quad f_0(0) = 0, \quad f'_0(0) = 1 \quad f'_0 \rightarrow 0 \text{ as } \eta \rightarrow \infty, \tag{34}$$

and for $k \geq 1$ we have

$$L_1[f_k(\eta)] = \chi_k L_1[f_{k-1}(\eta)] + c_0 \mathcal{D}_{k-1}^1(\eta), \quad f_k(0) = 0, \quad f'_k(0) = 0, \quad f'_k \rightarrow 0 \text{ as } \eta \rightarrow \infty, \tag{35}$$

where

$$\chi_k = \begin{cases} 0, & k \leq 1, \\ 1, & k \geq 1. \end{cases} \tag{36}$$

Here \mathcal{D}_k^ξ , for $\xi = 1, 2, 3$, is the homotopy derivative defined to be

$$\mathcal{D}_{k-1}^\xi(\eta) = \frac{1}{(k-1)!} \left(\frac{\partial^{k-1}}{\partial q^{k-1}} N_\xi \left[\sum_{j=0}^{\infty} f_j(\eta)q^j, \sum_{j=0}^{\infty} \theta_j(\eta)q^j \right] \right) \Big|_{q=0}. \tag{37}$$

Similarly, substituting (31)-(33) into (29) and (30) obtained:

$$L_2[\theta_0(\eta)] = 0, \quad \theta_0(0) = 1, \quad \theta_0 \rightarrow 0 \text{ as } \eta \rightarrow \infty, \tag{38}$$

$$L_3[\phi_0(\eta)] = 0, \quad \phi_0(0) = 1, \quad \phi_0 \rightarrow 0 \text{ as } \eta \rightarrow \infty, \tag{39}$$

and for $k \geq 1$

$$L_2[\theta_k(\eta)] = \chi_k L_2[\theta_{k-1}(\eta)] + c_1 \mathcal{D}_{k-1}^2(\eta), \quad \theta_k(0) = 0, \quad \theta_k \rightarrow 0 \text{ as } \eta \rightarrow \infty. \tag{40}$$

$$L_3[\phi_k(\eta)] = \chi_k L_3[\phi_{k-1}(\eta)] + c_1 \mathcal{D}_{k-1}^3(\eta), \quad \phi_k(0) = 0, \quad \phi_k \rightarrow 0 \text{ as } \eta \rightarrow \infty. \tag{41}$$

Using Liao's Method of Directly Defined Inverses, the deformation equations (35) and (40)-(41) are

$$f_k(\eta) = \chi_k f_{k-1}(\eta) + c_0 \mathcal{I} [\mathcal{D}_{k-1}^1(\eta)] + a_{k,1}e^{-\delta\eta} + a_{k,0}, \tag{42}$$

$$\theta_k(\eta) = \chi_k \theta_{k-1}(\eta) + c_1 \mathcal{I} [\mathcal{D}_{k-1}^2(\eta)] + b_{k,1}e^{-\delta\eta} + b_{k,0}, \tag{43}$$

$$\phi_k(\eta) = \chi_k \phi_{k-1}(\eta) + c_1 \mathcal{I} [\mathcal{D}_{k-1}^3(\eta)] + c_{k,1}e^{-\delta\eta} + c_{k,0}. \tag{44}$$

The benefit of the Optimal Homotopy Analysis Method is that it has a great freedom to choose the auxiliary linear operators L_1, L_2 and L_3 and initial guesses $f_0(\eta), \theta_0(\eta), \phi_0(\eta)$. After auxiliary linear operator and initial guesses are properly chosen we are free to determine how many terms $f_k, \theta_k, \phi_k \in V$ we want and can do iteratively. There has been great success in solving systems of nonlinear differential equations using OHAM (see [4]- [17]).

The only drawback of this homotopy analysis method is spending a lot of CPU time. First we choose auxiliary linear operators, and then solving the linear higher order deformation equation only to find out the inverse operators and applying them to quickly-growing expressions. However, in the latest innovation of Liao we have the freedom to directly define inverse operator by completely neglecting the linear operator. So, using this novel method can solve higher order deformation equations quickly and it's unnecessary to calculate inverse linear operators.

In our work the inversely defined mapping, \mathcal{J} , is the same for all three equations. But different directly defined inverses could be chosen if a different structure for the solutions f, θ and ϕ is required.

Define $\mathcal{J} : U \rightarrow V$ by

$$\mathcal{J} \left[e^{-k\delta\eta} \right] = \frac{e^{-k\delta\eta}}{Ak^3 + k}, \quad (45)$$

where A, δ are parameters which will be used to optimize the square residual error functions.

3 Results and Error Analysis

The appropriate solutions for the system (10)-(12) with boundary conditions (13)-(14) are obtained using MDDiM. Further used error analysis to get a general idea of how good the approximations are.

Define three term approximation $\hat{f}, \hat{\theta}$ and $\hat{\phi}$ which is sum of the first three solutions to the deformation equations. If they are exact, then they solve system (10)-(12), i.e., if $N_1[\hat{f}, \hat{\theta}, \hat{\phi}] = 0, N_2[\hat{f}, \hat{\theta}, \hat{\phi}] = 0$ and $N_3[\hat{f}, \hat{\theta}, \hat{\phi}] = 0$, then the three term approximations are exact solutions. If not $N_1[\hat{f}, \hat{\theta}, \hat{\phi}], N_2[\hat{f}, \hat{\theta}, \hat{\phi}]$ and $N_3[\hat{f}, \hat{\theta}, \hat{\phi}]$ become residual error functions that can be evaluated at any point η in the domain of the problem. Taking square of the L^2 -norm of error functions and setting converge control parameters to be $c_0 = c_2 = c_3$ define square residual error functions

$$E_\xi(Le, Nb, Pr, Nt, n, A, c_0, \delta) = \int_0^\infty \left(N_\xi[\hat{f}(\eta), \hat{\theta}(\eta), \hat{\phi}(\eta)] \right)^2 d\eta, \quad (46)$$

for $\xi = 1, 2, 3$. Since we have three error functions we will take affine combination of them as

$$E(Le, Nb, Pr, Nt, n, A, c_0, \delta) = \sum_{\xi=1}^3 E_\xi(Le, Nb, Pr, Nt, n, A, c_0, \delta). \quad (47)$$

But in practice the evaluation of $E_\xi(Le, Nb, Pr, Nt, n, A, c_0, \delta)$ is much time consuming so instead of exact residual error we use average residual error defined as

$$\hat{E}_\xi(Le, Nb, Pr, Nt, n, A, c_0, \delta) = \frac{1}{M+1} \sum_{j=0}^M \left(N_\xi[\hat{f}(j), \hat{\theta}(j), \hat{\phi}(j)] \right)^2. \quad (48)$$

Now, we minimize error functions with respect to A, c_0, δ and obtained optimal values of A, c_0, δ . Substituting those values in to $\hat{f}, \hat{\theta}$ and $\hat{\phi}$ we get three term approximation solution to the system (10)-(12) which satisfies

the conditions (13)-(14).

We start with initial guesses $f_0(\eta)$, $\theta_0(\eta)$ and $\phi_0(\eta)$ that satisfy the boundary conditions (13)-(14), respectively. We choose

$$f_0(\eta) = \frac{1}{\delta} - \frac{1}{\delta} e^{-\delta\eta}, \tag{49}$$

$$\theta_0(\eta) = e^{-\delta\eta}, \tag{50}$$

and

$$\phi_0(\eta) = e^{-\delta\eta}. \tag{51}$$

Now, using the deformation equations (42)-(44) to find $f_1(\eta)$, $\theta_1(\eta)$ and $\phi_1(\eta)$, they are

$$f_1(\eta) = -\frac{1}{2} \frac{c_0(n-1)}{(n+1)(4A+1)} + \frac{c_0(n-1)}{(n+1)(4A+1)} e^{-\delta\eta} - \frac{1}{2} \frac{c_0(n-1)}{(n+1)(4A+1)} e^{-2\delta\eta}, \tag{52}$$

$$\theta_1(\eta) = \frac{1}{2} \frac{(1+Nt \cdot \delta^2 + Nb \cdot \delta^2)c_0 \cdot \delta^2}{4A+1} e^{-\delta\eta} + \frac{1}{2} \frac{(1+Nt \cdot \delta^2 + Nb \cdot \delta^2)c_0 \cdot \delta^2}{4A+1} e^{-2\delta\eta}, \tag{53}$$

and

$$\phi_1(\eta) = -\frac{1}{4} \cdot \frac{Le \cdot c_0}{4A+1} e^{-\delta\eta} + \frac{1}{4} \cdot \frac{Le \cdot c_0}{4A+1} e^{-2\delta\eta}. \tag{54}$$

Using only three terms, let $\hat{f}(\eta) = f_0(\eta) + f_1(\eta) + f_2(\eta)$, $\hat{\theta}(\eta) = \theta_0(\eta) + \theta_1(\eta) + \theta_2(\eta)$ and $\hat{\phi}(\eta) = \phi_0(\eta) + \phi_1(\eta) + \phi_2(\eta)$, the sum of the square residual error function is given by

$$E(A, c_0, \delta) = \frac{1}{500} \sum_{j=0}^{499} \left(\sum_{\xi=1}^3 \left(N_{\xi} \left[\hat{f}(j), \hat{\theta}(j), \hat{\phi}(j) \right] \right) \right)^2. \tag{55}$$

and it is a function of A, c_0 and δ with parameters Le, Nb, Pr, Nt and n in it.

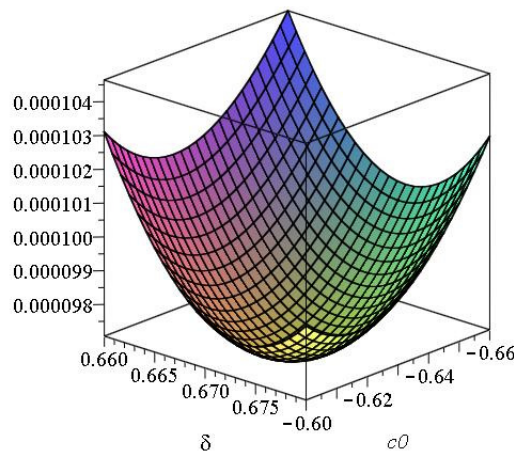


Fig. 2 Plot of $E(c_0, \delta)$, the squared residual error over $\eta \in [0, 499]$ as a function of c_0 and δ using parameter values $Le = 2, Nb = 2, Pr = 1, Nt = 1, n = 0.5, A = 0.1314$. The error function has minimum $E(c_0, \delta, A) = 9.71 \times 10^{-5}$ where $c_0 = -0.6195$ and $\delta = 0.8462963$.

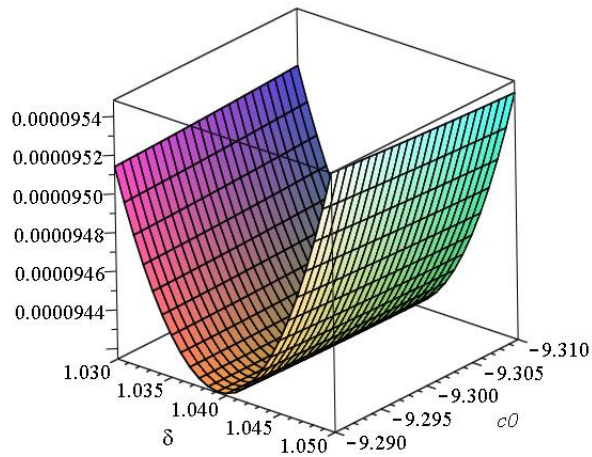


Fig. 3 Plot of $E(c_0, \delta)$, the squared residual error over $\eta \in [0, 499]$ as a function of c_0 and δ using parameter values $Le = 3, Nb = 1, Pr = 5, Nt = 0, n = 1, A = 7.8902$. The error function has minimum $E(c_0, \delta, A) = 9.41 \times 10^{-5}$ where $c_0 = -9.30195$ and $\delta = 1.03944$.

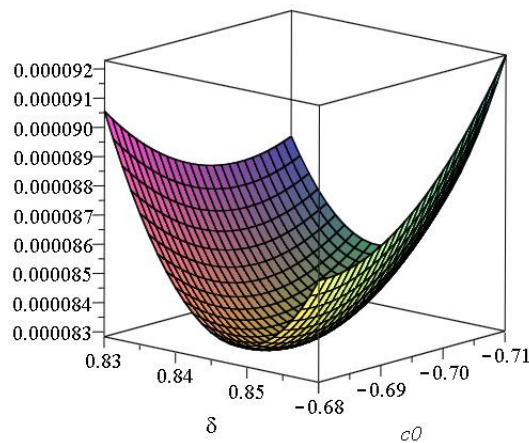


Fig. 4 Plot of $E(c_0, \delta)$, the squared residual error over $\eta \in [0, 499]$ as a function of c_0 and δ using parameter values $Le = 2, Nb = 2, Pr = 7, Nt = 0.5, n = 0.8, A = 0.24764$. The error function has minimum $E(c_0, \delta, A) = 8.28 \times 10^{-5}$ where $c_0 = -0.690605$ and $\delta = 0.8462963$.

Using three different sets of values for the parameters Le, Nb, Pr, Nt and n we found the sum of the square residual error $E(A, c_0, \delta)$ and are presented below.

Table 1 Minimum of the squared residual error $E(A, c_0, \delta)$ for three different sets of parameters.

Le	Nb	Pr	Nt	n	A	c_0	δ	$E(c_0, \delta, A)$
2	2	1	1	0.5	0.1314	-0.6195	0.673	9.71×10^{-5}
3	1	5	0	1	7.8902	-9.3020	1.0394	9.71×10^{-5}
2	2	7	0.5	0.8	0.2476	-0.6906	0.8463	8.28×10^{-5}

The plot of the error functions $E(A, c_0, \delta)$ is given in Figures 2-4 for three schemes at their optimum A values.

The plots of $\widehat{f}(\eta)$ and $\widehat{f}'(\eta)$ are presented in Figures 5-6, for parametric values in Table 1 for $E_1(A, c_0, \delta)$. In Figures 7-8 the plots of $\widehat{\theta}(\eta)$ and $\widehat{\phi}(\eta)$ are presented for parametric values in Table 1 for $E(A, c_0, \delta)$.

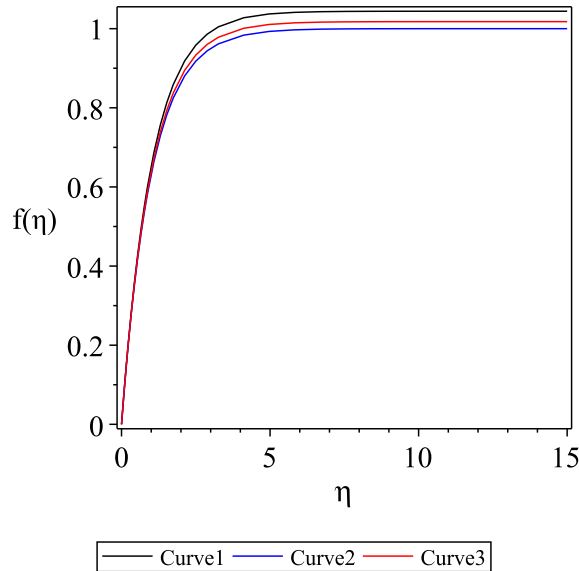


Fig. 5 Plot of $\widehat{f}(\eta)$, where Curve 1 has $Le = 2, Nb = 2, Pr = 1, Nt = 1, n = 0.5$, Curve 2 has $Le = 3, Nb = 1, Pr = 5, Nt = 0, n = 1$, and Curve 3 has $Le = 2, Nb = 2, Pr = 7, Nt = 0.5, n = 0.8$ using their respective error-minimizing convergence control parameter.

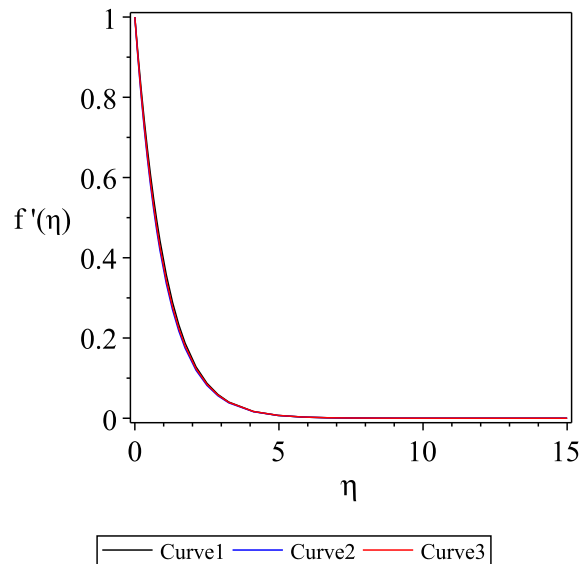


Fig. 6 Plot of $\widehat{f}'(\eta)$, where Curve 1 has $Le = 2, Nb = 2, Pr = 1, Nt = 1, n = 0.5$, Curve 2 has $Le = 3, Nb = 1, Pr = 5, Nt = 0, n = 1$, and Curve 3 has $Le = 2, Nb = 2, Pr = 7, Nt = 0.5, n = 0.8$ using their respective error-minimizing convergence control parameter.

A very good validation of the present analytical results has been achieved with the numerical results as shown in Figure 9. Also, it is found that the squared residual error decreases as a function of the number of

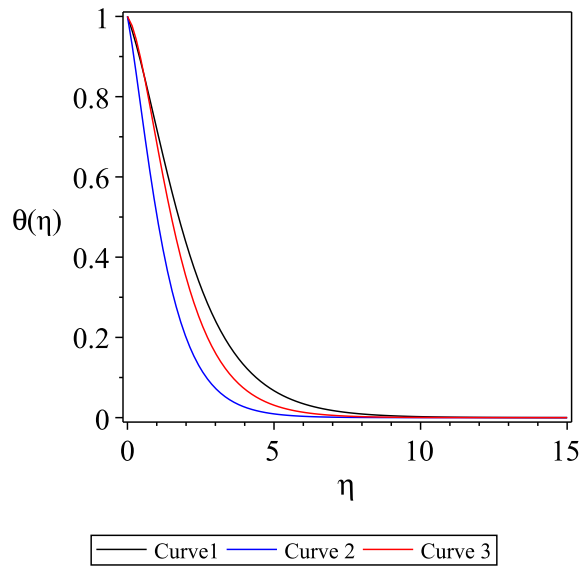


Fig. 7 Plot of $\hat{\theta}(\eta)$, where Curve 1 has $Le = 2, Nb = 2, Pr = 1, Nt = 1, n = 0.5$, Curve 2 has $Le = 3, Nb = 1, Pr = 5, Nt = 0, n = 1$, and Curve 3 has $Le = 2, Nb = 2, Pr = 7, Nt = 0.5, n = 0.8$ using their respective error-minimizing convergence control parameter.

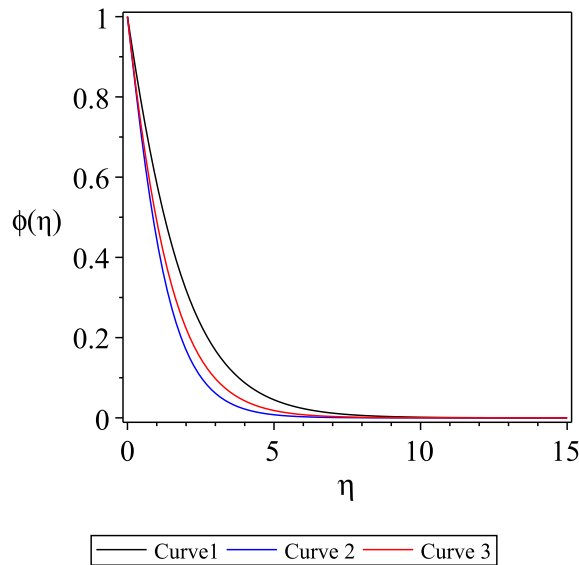


Fig. 8 Plot of $\hat{\phi}(\eta)$, where Curve 1 has $Le = 2, Nb = 2, Pr = 1, Nt = 1, n = 0.5$, Curve 2 has $Le = 3, Nb = 1, Pr = 5, Nt = 0, n = 1$, and Curve 3 has $Le = 2, Nb = 2, Pr = 7, Nt = 0.5, n = 0.8$ using their respective error-minimizing convergence control parameter.

terms in the approximation series, as shown in Figure 10.

The skin friction at the surface $|\hat{f}''(0)|$ as a function of the stretching parameter n is presented in Figure 11. It is found that skin friction decreases with an increase in stretching parameter. Figure 12 illustrated Nusselt number $|\hat{\theta}'(0)|$ as a function of Lewis number (Le) and Brownian motion parameter (Nb). It is found that Nusselt number decreases with increase Nt and Nb . Figure 13 illustrated Sherwood number $|\hat{\phi}'(0)|$ as a function of Nt, Nb and it is found that Sherwood number increases with increase Nt and but decreases with

increasing Nb .

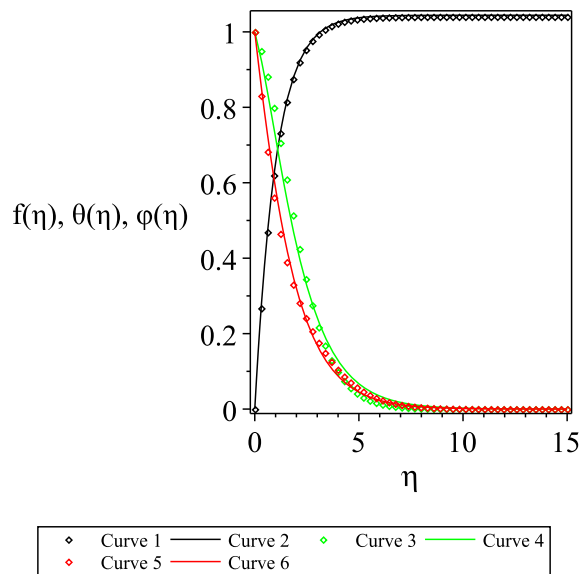


Fig. 9 Comparison of $f(\eta), \theta(\eta)$ and $\phi(\eta)$ obtained by the MDDiM 3-term approximation and shooting method solutions with $Le = 2, Nb = 2, Pr = 1, Nt = 1, n = 0.5$, where Curve 1 is shooting method results of $f(\eta)$, Curve 2 is MDDiM results of $f(\eta)$, Curve 3 is shooting method results of $\theta(\eta)$, Curve 4 is MDDiM results of $\theta(\eta)$, Curve 5 is shooting method results of $\phi(\eta)$, Curve 6 is MDDiM results of $\phi(\eta)$.

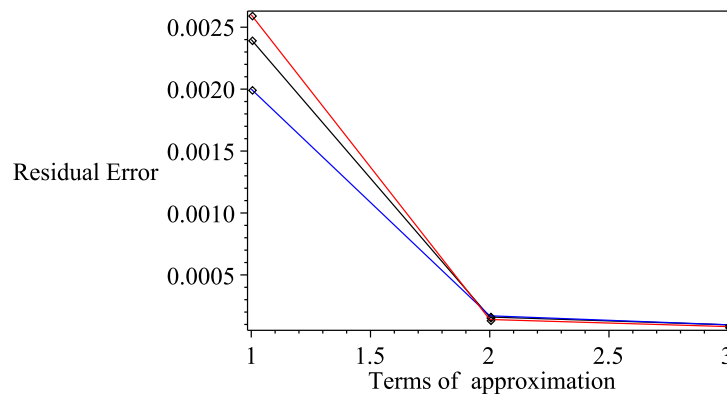


Fig. 10 Plot of Residual Error function versus Terms of approximation , where Curve 1 has $Le = 2, Nb = 2, Pr = 1, Nt = 1, n = 0.5$, Curve 2 has $Le = 3, Nb = 1, Pr = 5, Nt = 0, n = 1$, and Curve 3 has $Le = 2, Nb = 2, Pr = 7, Nt = 0.5, n = 0.8$ using their respective error-minimizing convergence control parameter.

4 Conclusions

Liao’s Directly Defining inverse Mapping method is extended to a system of three nonlinear differential equations. Approximate series solutions for $f(\eta), \theta(\eta)$, and $\phi(\eta)$ are obtained. Also, illustrated dimensionless velocity ($f(\eta)$), dimensionless temperature ($\theta(\eta)$) and dimensionless concentration ($\phi(\eta)$) profiles for three set of parameters (see Figures 5-8) are presented. Further, analytical results are compared with the numerical results (see Figure 9) and studied convergence of analytical results (see Figure 10).

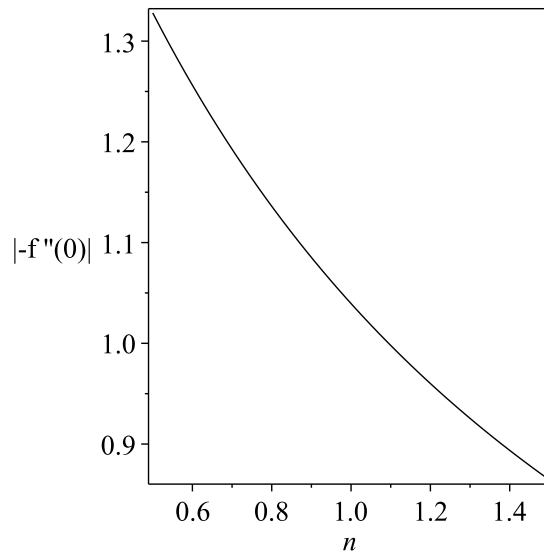


Fig. 11 Plot of $|\hat{f}''(0)|$ versus n , using $Le = 3, Nb = 1, Pr = 5$ and $Nt = 0$.

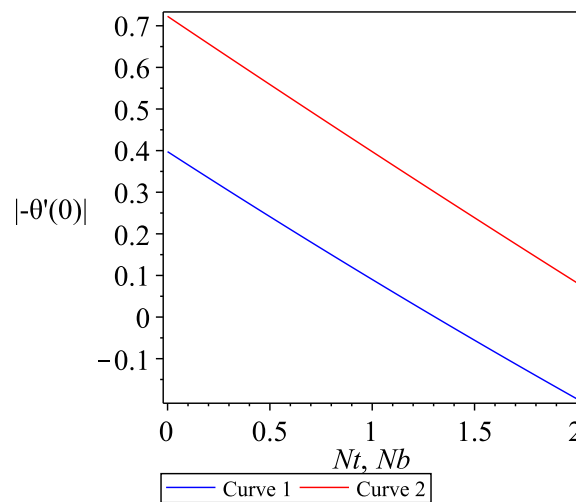


Fig. 12 Plot of $|\hat{\theta}'(0)|$, where Curve 1 is $|\hat{\theta}'(0)|$ versus Nt using $Le = 3, Nb = 1, Pr = 5, n = 1$, Curve 2 is $|\hat{\theta}'(0)|$ versus Nb using $Le = 3, Pr = 5, Nt = 0, n = 1$.

Since the inverse operator is directly defined, the series solutions are obtained with less CPU time. The freedom of choosing the inverse operator leads to obtaining less complicated terms for the approximation solution. Further, the selected inverse linear operator leads to three term solution which is accurate up to five decimal places by optimizing square residual function with respect to A, δ , and c_0 . Hence, we can conclude that MDDiM is not only easy to use, but also accurate. Theoretically, even if a smaller error was desired, it would just amount to computing more terms in the series by solving deformation equations. Furthermore, one can write an algorithm to iteration approach and truncate the approximate series solution at a given accuracy.

The idea is novel and is useful. This idea is not limited to a single nonlinear differential equation, but can be used for system of several equations. Also, it is important to note that finding an inverse operator that works well for the equation and it leads to an easily generated solution series. Hence, it is worth-while to investigate

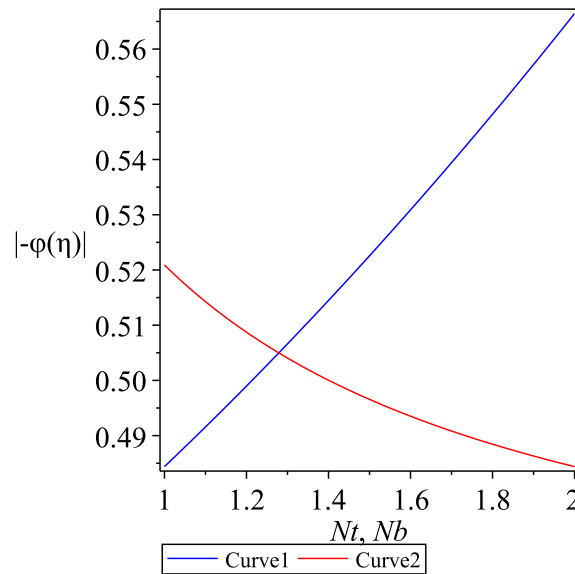


Fig. 13 Plot of $|-\hat{\phi}'(\eta)|$, where Curve 1 is $|-\hat{\phi}'(\eta)|$ versus Nt using $Le = 2, Nb = 2, Pr = 1, n = 0.5$, Curve 2 is $|-\hat{\phi}'(\eta)|$ versus Nb using $Le = 2, Pr = 1, Nt = 1, n = 0.5$.

this inverse linear operator.

Acknowledgements

The authors thank the reviewer for constructive and helpful comments that led to definite improvement in the paper.

References

- [1] P. Rana, R. Bhargava, 1. (2012), Flow and heat transfer of a nanofluid over a nonlinear stretching sheet: A numerical study, *Communication in Nonlinear Science and Numerical Simulation* 17, 212-226. doi [10.1016/j.cnsns.2011.05.009](https://doi.org/10.1016/j.cnsns.2011.05.009)
- [2] S. Liao, Y. Zhao, 2. (2016), Flow and heat transfer of a nanofluid over a nonlinear stretching sheet: A numerical study, *Communication in Nonlinear Science and Numerical Simulation*, 72.4, 989-1020. doi [10.1007/s11075-015-0077-4](https://doi.org/10.1007/s11075-015-0077-4)
- [3] M. Baxter, M. Dewasurendra, K. Vajravelu, 3. (2017), A method of directly defining the inverse mapping for solutions of coupled systems of nonlinear differential equations, *Numerical Algorithms*, 1-13. doi [10.1007/s11075-017-0359-0](https://doi.org/10.1007/s11075-017-0359-0)
- [4] S.J. Liao, 4. (2003), *Beyond Perturbation: Introduction to the Homotopy Analysis Method*, Chapman & Hall/CRC Press, Boca Raton.
- [5] S.J. Liao, 5. (2012), *Homotopy Analysis Method in Nonlinear Differential Equations*. Springer & Higher Education Press, Heidelberg, 2012. doi [10.1007/978-3-642-25132-0](https://doi.org/10.1007/978-3-642-25132-0)
- [6] R.A. Van Gorder and K. Vajravelu, 6. (2009), On the selection of auxiliary functions, operators, and convergence control parameters in the application of the Homotopy Analysis Method to nonlinear differential equations: A general approach, *Communications in Nonlinear Science and Numerical Simulation*, 14, 4078-4089. doi [10.1016/j.cnsns.2009.03.008](https://doi.org/10.1016/j.cnsns.2009.03.008)
- [7] K. Vajravelu and R.A. Van Gorder, 7. (2013), *Nonlinear Flow Phenomena and Homotopy Analysis: Fluid Flow and Heat Transfer*. Springer, Heidelberg. doi [10.1007/978-3-642-32102-3](https://doi.org/10.1007/978-3-642-32102-3)
- [8] R.A. Van Gorder, 8. (2012), Gaussian waves in the Fitzhugh-Nagumo equation demonstrate one role of the auxiliary function $H(x)$ in the homotopy analysis method, *Communications in Nonlinear Science and Numerical Simulation*, 17, 1233-1240. doi [10.1016/j.cnsns.2011.07.036](https://doi.org/10.1016/j.cnsns.2011.07.036)
- [9] M. Baxter, R.A. Van Gorder and K. Vajravelu, 9. (2014), On the choice of auxiliary linear operator in the optimal homotopy analysis of the Cahn-Hilliard initial value problem, *Numerical Algorithms*, 66, 269-298. doi [10.1007/s11075-013-9733-8](https://doi.org/10.1007/s11075-013-9733-8)

- [10] M. Baxter and R.A. Van Gorder, 10. (2014), Exact and analytical solutions for a nonlinear sigma model, *Mathematical Methods in the Applied Sciences*, 37, 1642-1651. doi [10.1002/mma.2926](https://doi.org/10.1002/mma.2926)
- [11] Y. Tan and S. Abbasbandy, 11. (2008), Homotopy analysis method for quadratic Riccati differential equation, *Communications in Nonlinear Science and Numerical Simulation*, 13, 539-546. doi [10.1016/j.cnsns.2006.06.006](https://doi.org/10.1016/j.cnsns.2006.06.006)
- [12] S. Liao, 12. (2010), An optimal homotopy-analysis approach for strongly nonlinear differential equations, *Communications in Nonlinear Science and Numerical Simulation*, 15, 2315-2332. doi [10.1016/j.cnsns.2009.09.002](https://doi.org/10.1016/j.cnsns.2009.09.002)
- [13] M. Baxter, R.A. Van Gorder and K. Vajravelu, 13. (2014), Optimal analytic method for the nonlinear Hasegawa-Mima equation, *The European Physical Journal Plus*, 129, 98. doi [10.1140/epjp/i2014-14098-x](https://doi.org/10.1140/epjp/i2014-14098-x)
- [14] R.A. Van Gorder, 14. (2014), Stability of the Auxiliary Linear Operator and the Convergence Control Parameter in the Homotopy Analysis Method. *Advances in the Homotopy Analysis Method*. Ed. S.-J. Liao. World Scientific, 123-180. doi [10.1142/9789814551250_0004](https://doi.org/10.1142/9789814551250_0004)
- [15] K. Mallory and R.A. Van Gorder, 15. (2014), Optimal homotopy analysis and control of error for solutions to the non-local Whitham equation, *Numerical Algorithms*, 66, 843-863. doi [10.1007/s11075-013-9765-0](https://doi.org/10.1007/s11075-013-9765-0)
- [16] K. Vajravelu, R. Li, M. Dewasurendra, K.V. Prasad, 16. (2016), Mixed Convective Boundary Layer MHD Flow Along a Vertical Elastic Sheet, *International Journal of Applied and Computational Mathematics*, 1-18. doi [10.1007/s40819-016-0252-x](https://doi.org/10.1007/s40819-016-0252-x)
- [17] R.A. Van Gorder, 17. (2016), Analytical method for the construction of solutions to the Föppl-von Kármán equations governing deflections of a thin flat plate, *International Journal of Non-linear Mechanics*, 47, 1-6. doi [10.1016/j.ijnonlinmec.2012.01.004](https://doi.org/10.1016/j.ijnonlinmec.2012.01.004)